Heterogeneity of mutational mechanisms and modes of inheritance in auriculocondylar syndrome

Gordon, Christopher T.; Vuillot, Alice; Marlin, Sandrine; Gerkes, Erica; Henderson, Alex; AlKindy, Adila; Holder-Espinasse, Muriel; Park, Sarah S.; Omarjee, Asma; Sanchis-Borja, Mateo

Published in:
JOURNAL OF MEDICAL GENETICS

DOI:
10.1136/jmedgenet-2012-101331

Publication date:
2013

ORIGINAL ARTICLE

Heterogeneity of mutational mechanisms and modes of inheritance in auriculocondylar syndrome

Christopher T Gordon,[1] Alice Vuillot,[1] Sandrine Marlin,[2] Erica Gerkes,[3] Alex Henderson,[4] Adila AlKindy,[5] Muriel Holder-Espinasse,[6] Sarah S Park,[7] Asma Omarjee,[1] Mateo Sanchis-Borja,[1] Eya Ben Bdira,[1] Myriam Oufadem,[1] Birgit Sikkema-Raddatz,[3] Alison Stewart,[8] Rodger Palmer,[9] Ruth McGowan,[10] Florence Petit,[6] Bruno Delobel,[11] Michael R Speicher,[12] Paul Aurora,[13] David Kilner,[13] Philippe Pellerin,[14] Marie Simon,[15] Jean-Paul Bonnefont,[15] Edward S Tobias,[16] Sixto García-Miñaúr,[17] Maria Bitner-Glindzicz,[18] Pernille Lindholm,[19] Brigitte A Meijer,[20] Véronique Abadie,[21] Françoise Denoyelle,[22] Marie-Paule Vazquez,[23,24,25] Christa Rotky-Fast,[26] Vincent Couloigner,[27] Sébastien Pierrot,[27] Yves Manach,[27] Sylvain Breton,[28,29] Yvonne M C Hendriks,[30] Arnold Munnich,[1,15] Linda Jakobsen,[19] Peter Kroisel,[12] Angela Lin,[31] Leonard B Kaban,[32] Lina Basel-Vanagaite,[33,34,35] Louise Wilson,[9] Michael L Cunningham,[7,36] Stanislas Lyonnet,[1,15] Jeanne Amiel[1,15]

► Additional material is published online only. To view please visit the journal online (http://dx.doi.org/10.1136/jmedgenet-2012-101331).

For numbered affiliations see end of article.

Correspondence to
Dr Christopher T Gordon and Professor Jeanne Amiel, INSERM U781, Tour Lavoisier 2ème étage, Hôpital Necker-Enfants Malades, 149 rue de Sèvres, Paris 75015, France; chris.gordon@inserm.fr, jeanne.amiel@inserm.fr

CTG and AV contributed equally

Received 1 October 2012
Revised 6 December 2012
Accepted 7 December 2012
Published Online First
12 January 2013

To cite: Gordon CT, Vuillot A, Marlin S, *et al*. *J Med Genet* 2013;**50**: 174–186.

ABSTRACT

Background Auriculocondylar syndrome (ACS) is a rare craniofacial disorder consisting of micrognathia, mandibular condyle hypoplasia and a specific malformation of the ear at the junction between the lobe and helix. Missense heterozygous mutations in the phospholipase C, β 4 (*PLCB4*) and guanine nucleotide binding protein (G protein), α inhibiting activity polypeptide 3 (*GNAI3*) genes have recently been identified in ACS patients by exome sequencing. These genes are predicted to function within the G protein-coupled endothelin receptor pathway during craniofacial development.

Results We report eight additional cases ascribed to *PLCB4* or *GNAI3* gene lesions, comprising six heterozygous *PLCB4* missense mutations, one heterozygous *GNAI3* missense mutation and one homozygous *PLCB4* intragenic deletion. Certain residues represent mutational hotspots; of the total of 11 ACS *PLCB4* missense mutations now described, five disrupt Arg621 and two disrupt Asp360. The narrow distribution of mutations within protein space suggests that the mutations may result in dominantly interfering proteins, rather than haploinsufficiency. The consanguineous parents of the patient with a homozygous *PLCB4* deletion each harboured the heterozygous deletion, but did not present the ACS phenotype, further suggesting that ACS is not caused by *PLCB4* haploinsufficiency. In addition to ACS, the patient harbouring a homozygous deletion presented with central apnoea, a phenotype that has not been previously reported in ACS patients.

Conclusions These findings indicate that ACS is not only genetically heterogeneous but also an autosomal dominant or recessive condition according to the nature of the *PLCB4* gene lesion.

INTRODUCTION

Auriculocondylar syndrome (ACS; MIM 602483 and 614669) is a craniofacial disorder with the core symptoms variable micrognathia, mandibular condyle hypoplasia and a specific malformation of the external ear at the junction between the lobe and helix (ranging from an indentation between the two to complete separation), known as a 'question mark ear' (QME). Other features of variable frequency include prominent cheeks, microstomia, palatal anomalies, glossoptosis, pre- and postauricular tags, facial asymmetry, crowded teeth and hearing loss (HL) (reviewed in Kokitsu–Nakata *et al*[1]). QME can occur as an isolated anomaly (IQME; MIM 612798). ACS is extremely rare, with less than 50 cases (including IQME) reported.[1–27] A high degree of intrafamilial phenotypic variability has been reported, with several examples of incomplete penetrance.[4 24] The first locus for ACS was mapped to a large interval on chromosome 1.[2] Recently, exome sequencing of several ACS cases led to the identification of missense mutations in phospholipase C, β 4 (*PLCB4*) and in guanine nucleotide-binding protein (G protein), α inhibiting activity polypeptide 3 (*GNAI3*),[24] the latter gene falling within the previously mapped interval on chromosome 1. All mutations reported thus far fall within the catalytic domain of each protein, and were predicted by Rieder *et al*[24] to result in dominant negative (PLCB4) or gain-of-function (GNAI3) proteins. Both proteins are predicted to function downstream of endothelin receptor type A, a G protein-coupled receptor in the endothelin 1 (EDN1) signalling pathway, which is known to play a crucial role in branchial arch patterning (reviewed in Clouthier *et al*[28]). Missense mutations in the catalytic domain of plcb3 (a homologue of PLCB4) were identified in the zebrafish mutant schmerle, which displays a

reduction of anterior branchial arch cartilage elements, and *plcb3* was shown to interact genetically with *edn1*,[29] supporting the involvement of PLCB4 in EDN1-regulated branchial arch development in humans.

The molecular bases of IQME are currently unknown; these cases may represent a genetically distinct entity, but given the variable expressivity that exists in *PLCB4*/*GNAI3* mutation-positive ACS cases, mutations in these two genes may also underlie IQME. Also, it was recently proposed that a series of patients with heterogeneous disorders of the first and second branchial arches, some of which resembled mild oculoauriculovertebral spectrum (OAVS) or Goldenhar syndrome (GS; MIM 164210), could be classified within ACS.[30] In this report, we tested for mutations in *PLCB4* and *GNAI3* in classic ACS, and overlapping phenotypes, such as IQME and OAVS/GS. Our results suggest a narrow phenotypic spectrum for *PLCB4*/*GNAI3* mutations, with mutation-dependent modes of inheritance. Interestingly, central apnoea may be an additional feature associated with PLCB4 loss of function.

METHODS

Patient classification

Patients with ACS, QME or related phenotypes were identified from the literature and by dysmorphologists, and classified into the following categories: eight cases with clinical ACS (meeting the minimal criteria of QME, ranging from a minor indentation at the helix-lobe junction to complete separation of the lobe from the helix, and micro- and/or retrognathia), three cases of IQME, five cases of atypical ACS previously reported by McGowan *et al*,[30] six cases diagnosed as OAVS or GS, and four cases presenting non-syndromic auricular dysplasia (including microtia, bifid lobe or hypoplastic lobe) with or without mandibular dysplasia (table 1).

Sequencing

Sanger sequencing was performed according to standard techniques. In all patients, we sequenced *PLCB4* exons 13–17 and 21–25 (coding for the catalytic domain) and all eight coding exons of *GNAI3*. In ACS and IQME patients in whom mutations were not identified in the *PLCB4* catalytic domain or in *GNAI3*, we sequenced all remaining coding exons of *PLCB4*, the catalytic domain exons of *PLCB3* (exons 10–13 and 15–18), and all coding exons of *GNAQ* and *GNA11*. Primer sequences used for amplification of *PLCB4*, *GNAI3*, *PLCB3*, *GNAQ* and *GNA11* exons are listed in online supplementary table S1.

Microsatellite analysis

Amplification and analysis of microsatellites were performed by standard techniques. Primer sequences used for amplification of microsatellites are listed in online supplementary table S2. Homozygosity in the interval containing *PLCB4* was tested with microsatellites D20S851 (426 kb upstream of the *PLCB4* transcript variant 1 start site), D20S917 (falling within intron 2 of *PLCB4*) and BBS6 (1119 kb downstream of the *PLCB4* transcript variant 1 start site).

Comparative genomic hybridisation

Case 8 was tested for chromosomal anomalies using a 135K comparative genomic hybridisation (CGH) whole genome array (Roche Nimblegen), with data analysed using InfoQuant Fusion software. The single probe showing reduced signal within the deleted interval is at chr20:9 392 652 (these and subsequent genomic coordinates refer to genome assembly Hg19).

Mutation modelling

Crystal structures were visualised using UCSF Chimera V.1.6. A crystal structure for PLCB4 has not been reported; we therefore modelled the residues mutated in PLCB4 to the structure of its paralogue, PLCB3. Protein Data Bank structure IDs: GNAI3, 2ODE;[31] PLCB3, 3OHM.[32]

Web resources

Variant screening was performed using the dbSNP135 database via the UCSC browser (http://genome.ucsc.edu/), and at the Exome Variant Server (http://evs.gs.washington.edu/EVS/). Evolutionary conservation of affected residues was assessed using Multiz at the UCSC browser. The effect of mutations on protein function was predicted using PolyPhen-2 (http://genetics.bwh.harvard.edu/pph2/index.shtml). Chromosomal aberrations were identified at the DECIPHER database (http://decipher.sanger.ac.uk/).

RESULTS

In this report, we studied 27 cases (see table 1), and we identified seven new mutations in *PLCB4* or *GNAI3* (cases 1–7) and one novel homozygous intragenic deletion in *PLCB4* (case 8). We present further phenotypic information for one case with a previously published *PLCB4* mutation (case 9). No causal mutations were identified in cases 10–27. All mutations in cases 1–7 were absent from dbSNP135 and the Exome Variant Server, affected highly conserved residues, and were predicted probably damaging by PolyPhen-2. For each de novo case (cases 3, 4 and 6), analysis of at least 11 microsatellites was consistent with paternity.

Case 1 was previously reported as a familial case of IQME, affecting three generations.[18] In the proband and her affected father, we identified a heterozygous missense mutation in *PLCB4* on chromosome 20: c.1073A>T, p.Glu358Val (NCBI Reference Sequences: NM_000933.3 and NP_000924.3) (figure 1A). DNA was not available from the affected paternal grandfather. We identified the same mutation in the proband's sister, who presented no external auricular or mandibular anomalies, suggesting incomplete penetrance. Although no mandibular abnormalities were previously reported in this family, some degree of mandibular dysplasia may have been present in the affected grandfather (figure 1D in Shkalim *et al*[18]) and also in the father as an adult (permission was not granted to publish photographs). We have not been able to assess x-rays or scans of the mandible in this family. Catalytic domains of PLC enzymes are composed of two highly conserved subdomains: the X and Y domains (figure 5A). Glu358 falls with the X domain, and is predicted to be a calcium-binding residue within the active site ((http://www.ncbi.nlm.nih.gov/Structure/cdd/cddsrv.cgi?uid=176533) and see below for structural modelling).

Case 2. A description of the craniofacial features of case 2 has been previously published.[25] The authors labelled her phenotype as dysgnathia complex, and she presented with the core features of ACS including a crease between the lobe and helix, micrognathia and dysplastic temporomandibular joints upon radiography. Sequencing of *PLCB4* revealed the mutation c.1078G>A, p.Asp360Asn (figures 1B and 5A). We were unable to obtain parental data for case 2. As for the residue mutated in case 1 (Glu358), Asp360 is predicted to contact the active site calcium.

Case 3. In a previous report, the phenotype of case 3 was briefly described as unilateral QME and micrognathia (case 2 in Greig *et al*[23]). This patient's ear deformity consists of a subtle

Table 1 Summary of key phenotypic features of patients tested for *PLCB4* and *GNAI3* mutations in the present report, and their respective genotypes

	Publication	Initial diagnosis	Gender	QME	Other auricular dysplasia	PoAT or PrAT	Micro- and/or retrognathia	Facial asymmetry	ED, CVD or CHD	Other phenotypes	Mutation	Inheritance
Case 1	Shkalim, 2008	Isolated QME	F	+	–	–	–	–	–	–	PLCB4, Glu358Val	Familial, AD
Case 2	Stuffken, 2008	DC (ACS)	F	+	–	–	+	–	–	–	PLCB4, Asp360Asn	?
Case 3	Greig, 2012 (case 2)	ACS	M	+	–	–	+	–	–	–	PLCB4, Asp360Val	Sporadic, AD
Case 4	Gerkes, 2008	ACS	M	+	–	PoAT	+	–	–	–	PLCB4, Arg621Cys	Sporadic, AD
Case 5	Present report	ACS	F	+	–	PoAT	+	–	–	–	PLCB4, Arg621Leu	Familial, AD
Case 6	Present report	ACS	M	+	–	–	+	–	–	Hypotonia	PLCB4, Arg621His	Sporadic, AD
Case 7	Present report	ACS	F	+	–	–	+	+	–	–	GNAI3, Ser47Arg	Familial, AD
Case 8	Present report	ACS	M	+	–	PoAT	+	–	–	Central apnoea, macropenis	PLCB4, IHD	Sporadic, AR
Case 9	Rieder, 2012 (case M003)	ACS	M	+	–	PoAT	+	–	–	Hamartomatous pedicles, CP	PLCB4, Arg621Cys	Familial, AD
Case 10	Present report	ACS	M	+	+	–	+	–	–	Bifid uvula, laryngeal cleft	–	Familial, AR?
Case 11	Present report	Isolated QME	F	+	–	–	–	–	–	–	–	Familial, AD
Case 12	Present report	Isolated QME	F	+	–	–	–	–	–	–	–	Familial, AD
Case 13	McGowan, 2011 (case 1)	GS then ACS	F	–	+	PrAT	+	–	–	Microcephaly, CP, HL	–	Sporadic, AD
Case 14	McGowan, 2011 (case 3)	GS then ACS	F	–	+	PrAT	+	+	–	HL	–	Sporadic, AD
Case 15	McGowan, 2011 (case 4)	TCS then ACS	F	–	+	PrAT	+	+	–	HL	–	Familial, AD
Case 16	McGowan, 2011 (case 5)	ACS	F	–	+	PrAT	+	+	–	–	–	Familial, AD
Case 17	McGowan, 2011 (case 6)	ACS	M	–	+	PrAT	+	+	–	Macroglossia	–	Familial, AD
Case 18	Present report	OAVS/GS	F	–	+	PrAT	+	+	ED, CVD, CHD	–	–	Sporadic, AD
Case 19	Present report	OAVS/GS	M	–	+	PrAT	+	+	ED	HL	–	?
Case 20	Present report	OAVS/GS	F	–	+	PrAT	+	+	CVD, CHD	Eyelid coloboma, FP	–	Sporadic, AD
Case 21	Present report	OAVS/GS	M	–	+	–	–	–	CHD	Cryptorchidism, FP	–	Sporadic, AD
Case 22	Present report	OAVS/GS	M	–	+	PrAT	+	–	ED, CVD, CHD	Renal hypoplasia	–	Sporadic, AD
Case 23	Present report	OAVS/GS	M	–	+	PrAT	–	+	CHD	–	–	Sporadic, AR?
Case 24	Present report	?	M	–	+	–	+	–	–	CP, HL	–	Sporadic, AD
Case 25	Present report	?	M	–	+	–	–	–	–	–	–	?
Case 26	Present report	?	M	–	+	?	?	?	?	?	–	?
Case 27	Present report	?	M	–	+	–	+	–	–	Absent uvula	–	Familial, AD

Note that phenotypic information is only provided for the proband of familial cases. ACS, auriculocondylar syndrome; AD, autosomal dominant; AR, autosomal recessive; CHD, congenital heart defect; CP, cleft palate; CVD, cervical vertebral defect; DC, dysgnathia complex; ED, epibulbar dermoid; FP, facial paralysis; GS, Goldenhar syndrome; HL, hearing loss; IHD, intragenic homozygous deletion; OAVS, oculoauriculovertebral spectrum; PoAT, postauricular tag; PrAT, preauricular tag(s); QME, question mark ears; TCS, Treacher Collins syndrome; ?, no information available.

notch at the junction between lobe and helix, and is therefore at the mildest end of the QME spectrum. A CT scan revealed severe bilateral condylar hypoplasia and dysmorphic ramus/condyle units. An initial sleep study indicated predominantly obstructive apnoeas with total number of central apnoea (CA)/obstructive apnoea (OA)/mixed apnoea (MA)/hypopnea (H) events=6/21/2/53. In a subsequent sleep study performed after one of several distraction surgeries, the majority of apnoeas appeared central, occurring generally during rapid eye movement (REM) sleep or after arousals, although they were not deemed to be pathologic, with total CA/OA/MA/H events=26/0/0/1. Sequencing of the proband and his parents identified a de novo mutation in the proband in *PLCB4*: c.1079A>T, p.Asp360Val (figures 1C and 5A). This is the same calcium-binding residue mutated in case 2 above, although a different nucleotidic change.

Case 4 has been previously described,[9] and displays typical features of ACS. Postauricular tags were noted by Gerkes *et al*[9]; this feature is not frequently reported in the ACS literature, yet appears to be specific for this syndrome. We identified a de novo mutation in *PLCB4* in the proband: c.1861C>T, p.Arg621Cys, falling in the Y domain of the catalytic domain (figures 1D and 5A). Supporting this de novo mutation being causative, the parents presented no physical abnormalities, and had normal orthopantograms. This is exactly the same mutation identified by Rieder *et al*[24] in a familial ACS case (pedigree M003).

Case 5, from the UK, presented classic features of ACS, that is, QME (previously published as Figures 62c and 66a in Hunter *et al*[33]), severe micrognathia, large cheeks and microstomia (figure 2Ai–iii). She displayed over-folded helices and a large postauricular tag on her left ear. Her father has a small low-set right ear with a dysplastic and over-folded helix, without anomaly at the lobe-helix junction (figure 2Aiv–vi). An orthopantogram of the father revealed shorter than normal mandibular rami with a flattened head of the right condyle. The proband and her father harboured the *PLCB4* mutation c.1862G>T, p.Arg621Leu (figures 1E and 5A). We were unable to test whether the mutation arose de novo in the father, as his parents are no longer alive, but examination of photos did not suggest that they were affected.

Case 6 is from Oman. He presented with neonatal hypotonia, developmental delay, feeding difficulties and upper airway obstruction. He was diagnosed with ACS based on micrognathia (with hypoplastic mandibular ramus upon CT scan), full cheeks, microstomia, difficulties in opening the mouth and low-set QMEs (figure 2Bi–iii). A skin tag positioned anterior to the sternocleidomastoid may be a remnant of the left ear lobe completely detached from the pinna (figure 2Biii). He has had several distraction surgeries. Cardiovascular and ophthalmological examinations have been normal, and he is of normal intelligence. Sequencing of *PLCB4* identified the mutation c.1862G>A, p.Arg621His (figures 1F and 5A). The parents and brother of case 6 did not harbour the mutation. This is exactly the same mutation previously found in a large ACS family (M001 in Rieder *et al*[3 24]). Case 6 is the fifth independent ACS case with a mutation affecting Arg621, after case 4 in this report and M003 in Rieder *et al*[24] (both Arg621Cys), case 5 in this report (Arg621Leu), and M001 in Rieder *et al*[24] (Arg621His).

Case 7 presented with asymmetric micrognathia, malocclusion, microstomia and a notch between the lobe and helix of the right ear (figure 2Ci–iii). She also displayed mildly hypoplastic first ribs upon x-ray. She harboured a heterozygous missense mutation in *GNAI3* on chromosome 1: c.141C>A, p.Ser47Arg (NCBI Reference Sequences: NM_006496.3 and NP_006487.1) (figures 1G and 5A). The mutation was inherited from her father who had normal ears but large cheeks and possible hypoplasia of the angle of the mandible (figure 2Civ–vi). Mandibular x-rays were not available for the father. We were not able to obtain material to test for the mutation in the paternal grandparents. Several lines of evidence support the pathogenicity of this GNAI3 Ser47Arg mutation, including structural mapping (see below) and functional studies of mutations of the equivalent serine in other GTP-binding proteins (see Discussion).

Case 8 was born to healthy second-cousin parents of Indian descent, and presented with typical features of ACS, that is, micrognathia, microstomia, full cheeks, bilateral QME and a postauricular tag on the right ear (figure 3Ai). A CT scan demonstrated dysplastic condyles and shallow condylar fossae bilaterally. He has a significantly enlarged penis with descended testes, bilateral hydroceles and some hirsutism over his back. Brain MRI, echocardiogram, abdominal ultrasound, barium upper gastrointestinal (GI) study, neonatal hearing screen and ophthalmology assessment were all normal. He has ongoing swallowing problems, poor suck requiring a nasogastric tube and significant gastro-oesophageal reflux. Electromyography (EMG) sampling of the genioglossus and of the tibialis showed only chronic neurogenic changes in the tongue, suggesting a bulbar palsy. Shortly after birth, he displayed tachypnoea and a persistent oxygen requirement. Ear, nose and throat (ENT) examination showed some laryngomalacia. There was no evidence of obstruction, and mandibular elongation was not performed. Sleep studies were conducted due to recurrent profound apnoeas. In five out of six sleep studies, central apnoeas were more frequent than obstructive apnoeas: (1) CA/OA/MA/H events=106/9/0/14; (2) CA/OA/MA/H events=35/0/0/31; (3) CA/OA/MA/H events=88/1/1/5; (4) CA/OA/MA/H events=80/0/0/14; (5) CA/OA/MA/H events=291/14/1/40 and (6) CA/OA/MA/H events=39/141/29/2. Apnoeas were managed with intermittent BiPAP and ongoing supplemental oxygen. There were no obvious signs of ACS in the proband's parents (figure 3Aii, iii) nor in the maternal grandparents, who themselves are first cousins (figure 3B). Three of the mother's brothers died in childhood or young adulthood. Although they were not seen in the clinic, from photographic evidence, one appears to have had achondroplasia, the other two were not overtly dysmorphic but were intellectually deficient, and there were no visible ear malformations. Karyotype and array CGH at 0.2 Mb resolution did not reveal chromosomal anomalies in the proband. No mutations were identified in the *PHOX2B* coding region. Sequencing of *PLCB4* identified no mutation, although we were unable to amplify exons 21–24. Suspecting a homozygous deletion, we reduced the putative deletion interval by confirming the presence of a series of amplicons in introns 20 and 24 (amplicons a–d in figure 3C). Sequencing of a proband-specific product spanning from amplicon a to b demonstrated a deletion of 4997 bp (chr20:9388282–9393278) (figure 3C, D). Three base pairs of microhomology existed at the breakpoint; this is a common copy-number variant (CNV) breakpoint signature.[34] Retrospective examination of the *PLCB4* locus in two independent prior array CGH experiments indicated a reduced signal for the only probe within the deleted region, consistent with homozygous loss (figure 3E). In all three RefSeq *PLCB4* transcripts, the deletion is predicted to result in a frameshift and premature stop codon, and therefore, the proband should be homozygous null for *PLCB4*, assuming nonsense-mediated decay. Using the deletion-spanning primers for genotyping in each parent, we amplified the same deletion-spanning product

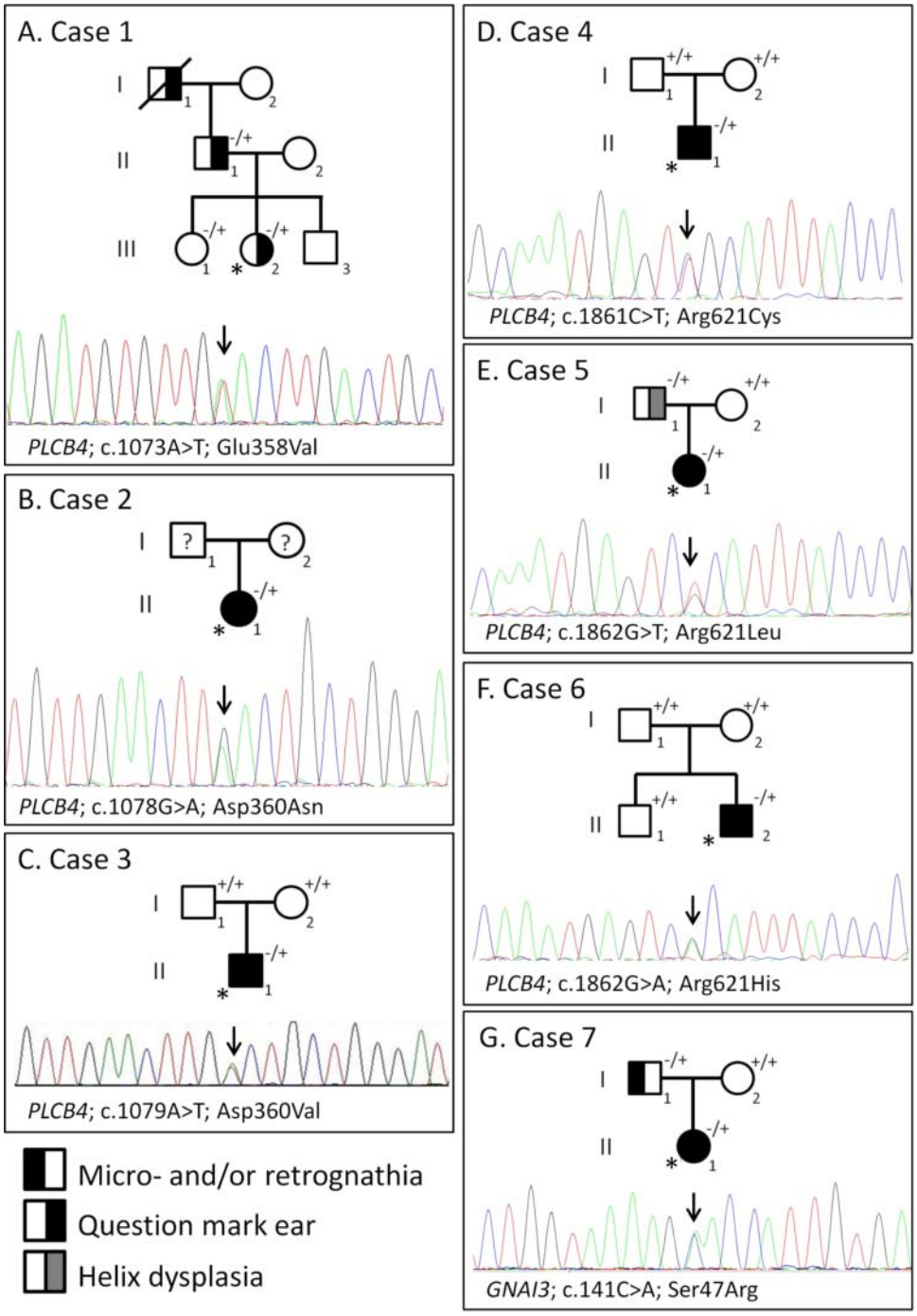

Figure 1 Identification of missense mutations in *PLCB4* and *GNAI3* in auriculocondylar syndrome patients. A mutant or wild-type allele is denoted by a minus or plus sign, respectively. A question mark indicates that no information was available. Each proband is indicated by an asterisk. This figure is only reproduced in colour in the online version.

of the proband, plus the wild-type product (figure 3F), indicating heterozygous intragenic deletion of *PLCB4* in each parent. Accordingly, the proband was homozygous for a haplotype at the locus (defined by microsatellites D20S851, D20S917 and BBS6) that was present in each parent in the heterozygous state.

Given the evidence for central apnoea in cases 3 and 8 above, we reassessed sleep studies that were performed for three of the ACS cases in Rieder *et al*.[24] Case S011 (GNAI3 p.Gly40Arg) in that report had a sleep study after distraction and decannulation at age 6 years, with CA/OA/MA/H events=5/14/6/0. Case S001 (PLCB4 p.Tyr623Cys) had a sleep study at age 6 years after distraction and decannulation (but later on needed the tracheostomy tube replaced), with CA/OA/MA/H events=26/19/0/0. Following successful distraction and decannulation, case S008 (GNAI3 p.Gly40Arg) had a sleep study with CA/OA/MA/H events=0/2/0/25.

All ACS-associated *PLCB4* point mutations reported here and in Rieder *et al*[24] are missense mutations clustered in the catalytic domain, suggesting that they may function as dominant negatives rather than haploinsufficient alleles. This is consistent with the absence of an ACS phenotype in the parents of case 8, who each carried a heterozygous deletion. To provide further support for this, we assessed the craniofacial phenotypes of patients with chromosomal aberrations disrupting *PLCB4*, entered in the

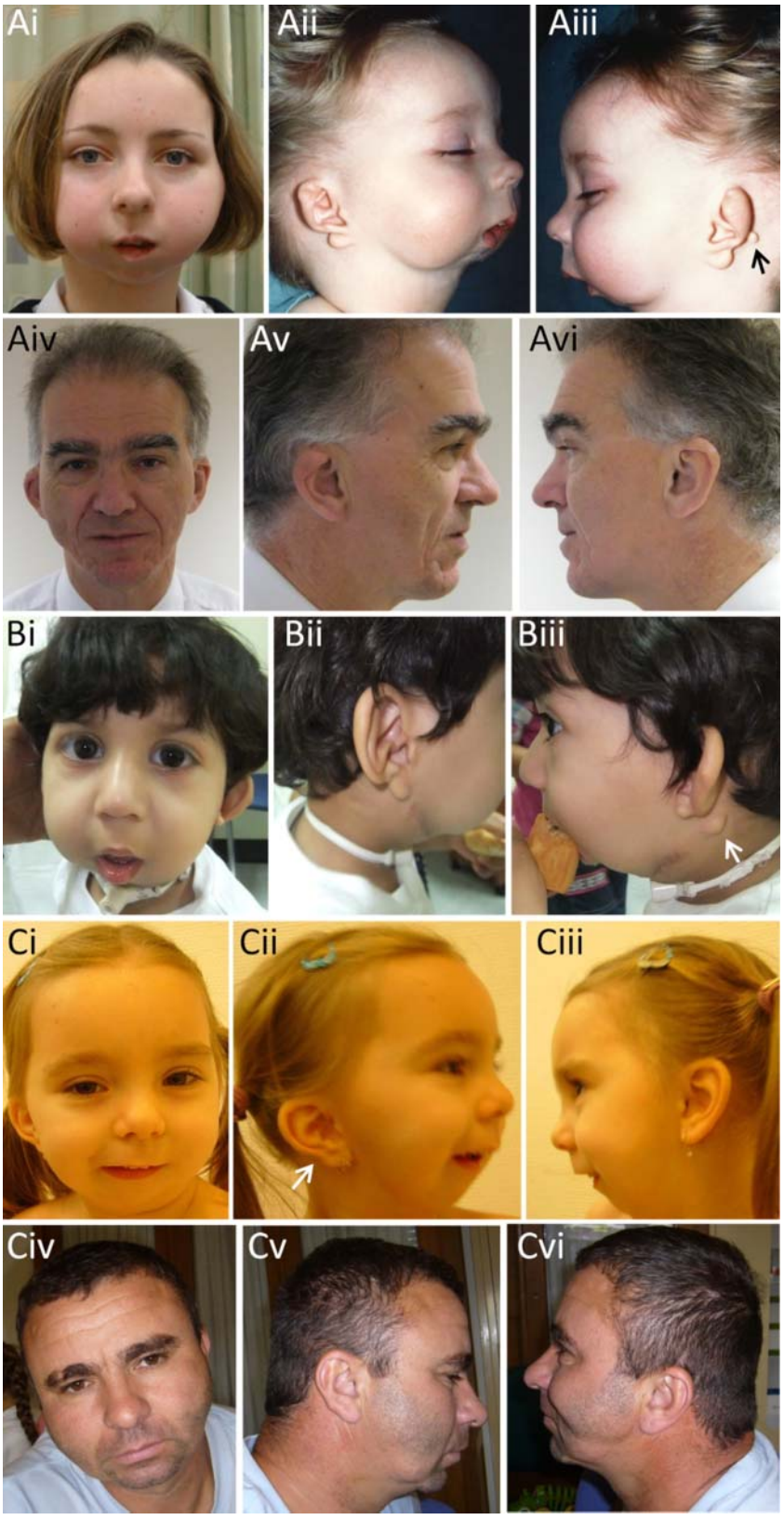

Figure 2 Craniofacial features of auriculocondylar syndrome patients harbouring PLCB4 or GNAI3 mutations. Ai–iii, case 5 (PLCB4 mutation Arg621Leu); Aiv–vi, case 5's father (PLCB4 mutation Arg621Leu). Bi–iii, case 6 (PLCB4 mutation Arg621His). Ci–iii, case 7 (GNAI3 mutation Ser47Arg); Civ–vi, case 7's father (GNAI3 mutation Ser47Arg). A large postauricular tag in Aiii is indicated by an arrow. The arrow in Biii indicates a large tag below the ear that may be a remnant of the ear lobe. An arrow in Cii indicates a notch in the external margin of the ear, at the junction between the helix and the lobe. This figure is only reproduced in colour in the online version.

DECIPHER database. DECIPHER patient 253 449 harbours a deletion (likely heterozygous, based on mean ratio of −1) at chr20:8 509 979–9 822 641, containing four genes, including *PLCB4* in its entirety, and an adjacent inverted duplication (chr20:126 054–8 131 005). This patient displayed no facial features suggestive of ACS. DECIPHER patient 1692 harbours a deletion (likely heterozygous, based on mean ratio of −0.7) at chr20:9 249 717–12 702 585, which includes most of *PLCB4*, and 10 other genes including *JAG1*, and consistent with *JAG1* haploinsufficiency the patient was diagnosed with Alagille syndrome. No auricular abnormalities or micrognathia were reported. Patient 2009 is reported as having a duplication

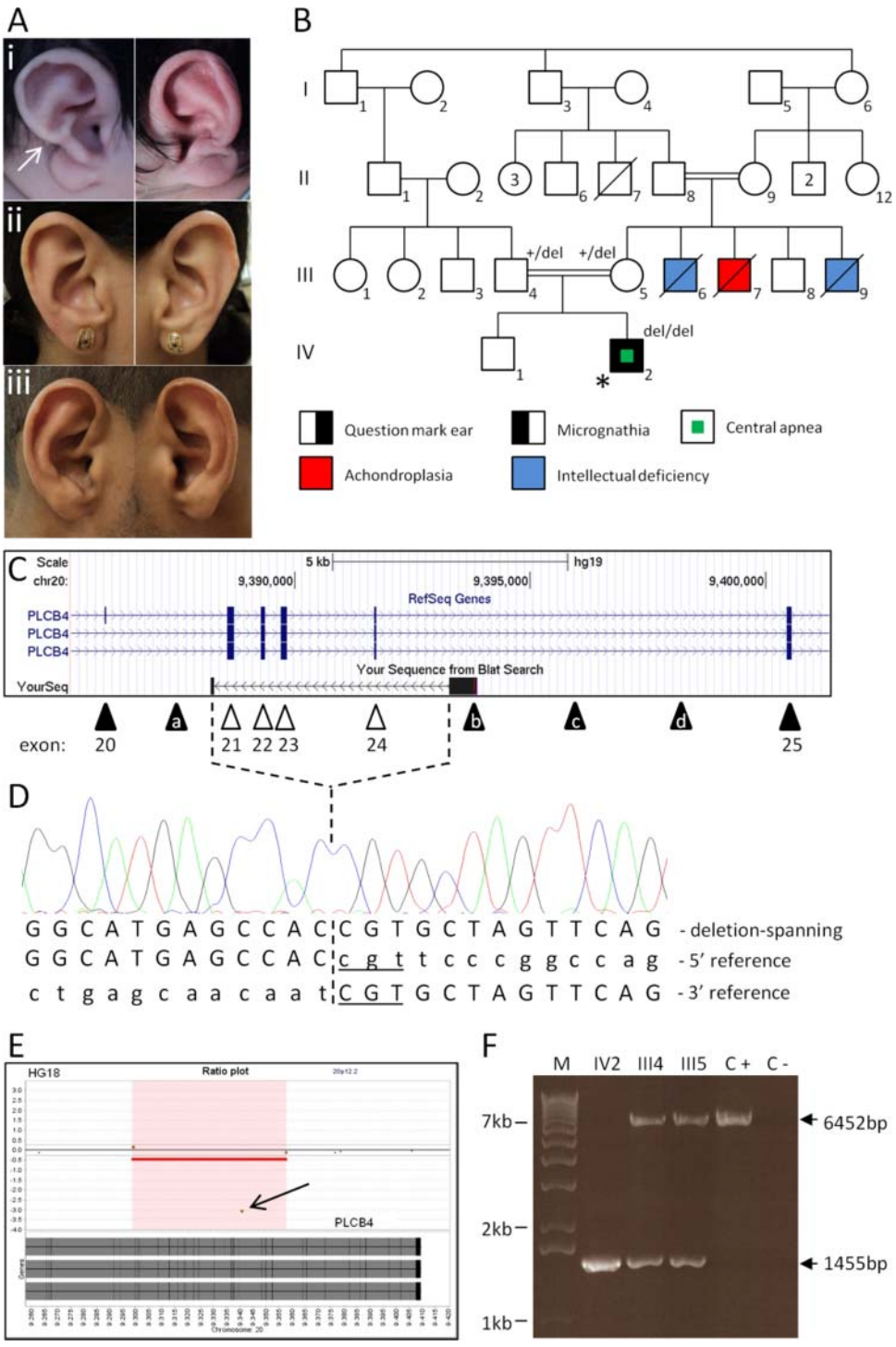

Figure 3 Identification of a homozygous deletion within *PLCB4* in case 8. (A) ears of the proband (i), his mother (ii) and his father (iii). An arrow in Ai indicates a small postauricular tag protruding from behind the helix. (B) case 8 pedigree. An asterisk indicates the proband. Note, that the only individuals seen in the clinic were II8, II9, III4, III5, IV1, IV2. The presence or absence of phenotypes in other family members is based on photographic evidence or as reported by the family. (C and D) localisation of the deletion breakpoints. Amplicons that could be obtained from the proband's DNA are indicated by black triangles (exons 20 and 25, and intronic amplicons a–d), while those unamplifiable are indicated by empty triangles (exons 21–24). The amplicons are depicted beneath a UCSC browser screenshot of the three *PLCB4* RefSeq transcripts. Forward and reverse primers from amplicons a and b, respectively, yielded a PCR product of 1455 bp from the proband's DNA, and the precise deletion breakpoints were obtained by sequencing this product with the amplicon b reverse primer. In D, a region of microhomology at the deletion breakpoints is underlined. Bases within the deleted region are in lowercase. (E) CGH array indicating loss of a single probe (arrow) within the deleted region. (F) PCR genotyping of the parents of case 8 using forward and reverse primers from amplicons a and b, respectively. Each parent (III4 and III5) yielded a wild-type product with expected size of 6452 bp, plus the deletion-containing product of 1455 bp. IV2, proband; C +, wild-type positive control DNA; C −, reaction without DNA; M, size marker. This figure is only reproduced in colour in the online version.

entirely within *PLCB4* (encompassing exons 3–24; this duplication may give rise to a frameshifted protein), inherited from a normal parent, and a de novo deletion on chr17—no auricular or mandibular phenotypes are listed for the patient. Patient 263 696 is listed with a duplication encompassing a 3′ part of *PLCB1* and a 5′ part of *PLCB4* (these genes are contiguous, and arranged tail (*PLCB1*) >head (*PLCB4*), 5′ >3′), inherited from a normal parent, with no other CNVs. The phenotypes listed for this patient are cryptorchid testes and unilateral absent auditory canal and ossicles. This is intriguing given that auditory canal atresia and stenosis and conductive HL have been reported in ACS patients,[2 3 5 15] and it would be worth investigating the possibility of an expressed *PLCB4-PLCB1* fusion transcript in patient 263 696. We were unable to obtain further details for these latter two DECIPHER cases. Finally, several interstitial deletions of 20p12 have been reported in the literature, with probable heterozygous loss of *PLCB4*, but without an associated ACS phenotype (see Discussion).

Case 9 corresponds to the familial case M003 in Rieder *et* al,[24] in which the PLCB4 mutation p.Arg621Cys was identified in the proband and his essentially asymptomatic father, while several relatives of the father were reported to display ACS-like features, without having been seen in the clinic. We present further details about the family that have come to light recently. The phenotype appears to have originated in the 13th and last child of the great-great-grandparents of the proband, suggestive of a neomutation on the paternal allele (figure 4A). We confirmed the presence of the p.Arg621Cys mutation in the paternal aunt (individual IV3). She presented, in contrast to her brother IV1 (figure 4C), ears typical of ACS (figure 4B), and had bilateral HL as a child but has a normal mandible. Typical ACS features can also be seen in individual III1 (figure 4D), who died at the age of 4 years from meningitis. The proband, in addition to a characteristic crease between the lobe and helix (figure 4E), displayed a postauricular tag (figure 4F) of a similar size and position to that of case 4 in the present report (see figure 3 in Gerkes *et al*[9]). A CT scan of the proband confirmed dysplasia of the mandibular ramus and condyle (figure 4G), and during surgery two hamartomatous pedicles were discovered in his throat; these may be similar in aetiology to previously reported soft tissue masses emanating from the posterior base of the mouth in ACS patients.[5 24]

Case 10 consists of an affected brother and sister born to healthy first-cousin parents. The brother presented with bifid uvula, laryngeal cleft, short velum, retrognathia, a typical QME on the right, a severely dysmorphic left ear and an aneurysm of the vein of Galen, while his sister displayed a left QME, overfolded helix on the right, glossoptosis and mandibular hypoplasia requiring distraction. Analysis of two microsatellites did not support homozygosity at the *PLCB4* locus in the affected children. No mutations were identified in the entire coding region of *PLCB4*, *GNAI3*, the catalytic domain exons of *PLCB3* (selected as a candidate given the branchial arch dysplasia in zebrafish harbouring *plcb3* mutations[29]), or the coding region of *GNAQ* and *GNA11*, encoding G α proteins required for mandibular development in mice.[35–38]

Case 11 is a familial case of IQME, originating from Armenia. The mother presented with a significant notch in the border of the helix, at the lobe-helix junction, bilaterally. Her daughter displayed bilateral clefting between the lobe and helix. No overt signs of mandibular hypoplasia were evident. x-rays of the mandible of the daughter at 2 years of age did not reveal any obvious anomalies. No mutations were identified in the complete coding region of *PLCB4*, *GNAI3*, *GNAQ*, *GNA11* or in the catalytic domain exons of *PLCB3*.

Case 12 consists of a mother, her daughter and her son, of African origin, all three presenting with IQME. The mother displayed a notch at the lobe-helix junction, and her son and daughter each had protruding helices and clefting, or constriction, between the lobe and helix. The daughter has been treated for acute lymphoblastic leukaemia. We were not able to assess mandibular x-rays in this family, but there were no external signs of micrognathia. We did not identify mutations in the complete coding region of *PLCB4*, *GNAI3*, *GNAQ*, *GNA11* or in the catalytic domain exons of *PLCB3*.

We also sequenced the catalytic domain exons of *PLCB4* and the coding region of *GNAI3* in cases 1, 3, 4, 5 and 6 in McGowan *et al*,[30] in six cases having been diagnosed as OAVS or GS, and in four cases with poorly defined ear dysplasias, including microtia or hypoplastic lobe, with or without mandibular dysplasia (cases 13–27 in table 1). No clearly pathogenic mutations were identified.

Mapping of mutated residues to protein structures

Previously, structural modelling of the four PLCB4 amino acid positions mutated in ACS patients indicated that they all occur within the catalytic domain (figure 5B and Rieder *et al*[24]). All four are predicted to form bonds with inositol triphosphate, the active-site calcium, or other amino acids involved in catalysis.[24] Mapping the two novel mutated residues in this report, Glu358 and Asp360, to the PLCB3 crystal structure indicated that both are predicted to contact the active-site calcium (figure 5B). All six PLCB4 residues now known to be mutated in ACS exhibit a striking clustering in protein space (figure 5B). Mapping of Ser47, a novel mutation of which was identified in case 7 of this report, to the GNAI3 crystal structure, indicated that it makes contact with the active-site magnesium, which in turn coordinates the positioning of GTP (figure 5C and see ref. [39]).

DISCUSSION

Following on from the initial description of *PLCB4* and *GNAI3* mutations in ACS, we tested both genes in several additional patients diagnosed with classic ACS, IQME, OAVS/GS and in others with less clearly defined auricular and mandibular dysplasias. Of 11 ACS/IQME patients tested, six harboured missense *PLCB4* mutations, one had a homozygous deletion within *PLCB4* predicted to result in complete loss of the protein, and one had a missense mutation in *GNAI3*. Combining the mutations reported here and in Rieder *et al*,[24] 12/15 solved cases (80%) have a *PLCB4* lesion, and 3/15 (20%) have a *GNAI3* mutation. Two PLCB4 amino acids emerge as hotspots: five out of the total of 11 *PLCB4* point mutations now described occur at Arg621 (Arg621Cys x 2, Arg621His x 2, Arg621Leu) and two occur at Asp360 (Asp360Asn, Asp360Val). When mapped to the PLCB3 crystal structure, these two and all other mutated PLCB4 residues are predicted to form bonds important for catalysis in the active site.

We have elucidated the molecular basis of the first recessive case of ACS. Case 8 harboured a homozygous deletion of four exons within *PLCB4*, predicted to result in complete loss of the protein, with each mutant allele inherited from his consanguineous, unaffected parents, each of whom was heterozygous for the deletion. We note that patient 2 in Guion–Almeida *et al*[5] was born to consanguineous parents and presented with ACS plus the atypical features of low birthweight, hypotonia, ptosis, downslanting palpebral fissures, learning disability and delayed neuropsychomotor and language development. The possibility of homozygous loss-of-function alleles would be worth investigating in this patient. ACS was evoked in another patient born to

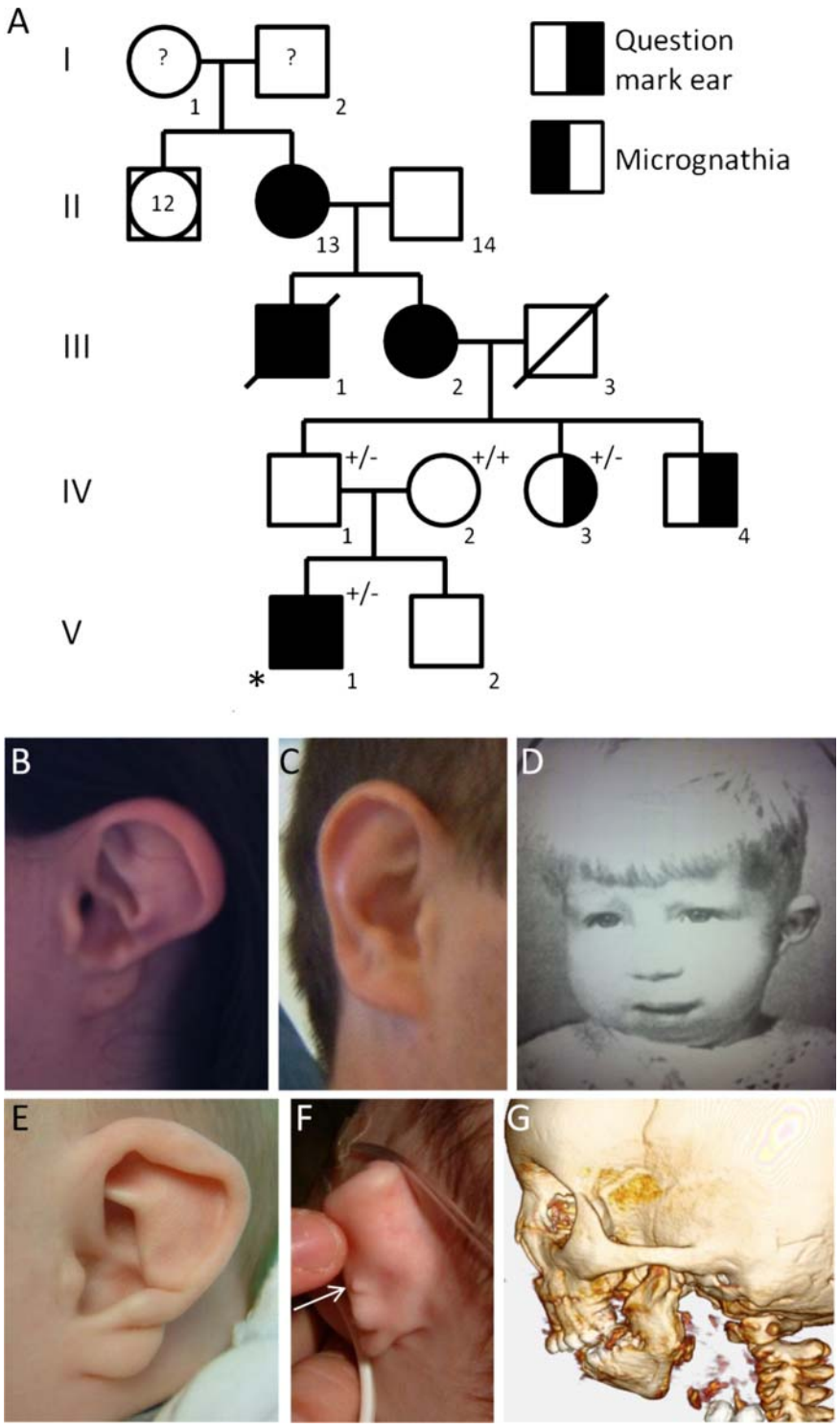

Figure 4 Inheritance and auricular features of case 9, harbouring the PLCB4 mutation Arg621Cys. (A) case 9 pedigree. The *PLCB4* mutant or wild-type allele is denoted by a minus or plus sign, respectively. A question mark indicates that no information was available. An asterisk indicates the proband. (B) individual IV3. (C) individual IV1. (D) individual III1. (E–G) individual V1, the proband. In (F) an arrow indicates the postauricular tag. (G) CT scan. This figure is only reproduced in colour in the online version.

consanguineous parents,[40] but in our opinion, this diagnosis is unlikely to be correct. In addition to ACS, the patient carrying a homozygous deletion described here presented with central apnoea in repeated sleep studies. Although respiratory distress and presumed obstructive apnoea are commonly reported in ACS patients, central apnoea has not been described. After this finding, we analysed sleep studies performed in other ACS patients, and we found evidence for central events in some cases after distraction surgery, a procedure that should reduce obstructive apnoea events and unmask central events, if present. The potential role of *PLCB4* in central control of respiration may be best addressed in *Plcb4* homozygous null mice, under conditions that challenge respiration. Drawing on evidence from animal models harbouring mutations in genes of the endothelin signalling pathway, Rieder *et al*[24] proposed that PLCB4 and GNAI3 may function downstream of endothelin signalling during branchial arch patterning. Interestingly, mutations in some endothelin signalling pathway components are associated with defects in respiratory control (reviewed in Gaultier *et al*[41]).

All previously described PLCB4 mutations were missense, clustered within the catalytic domain, and it was suggested that these mutations may result in dominant negative PLCB4 proteins.[24] Support for this idea comes from evidence suggesting that the plcb3 missense mutations in the zebrafish schmerle

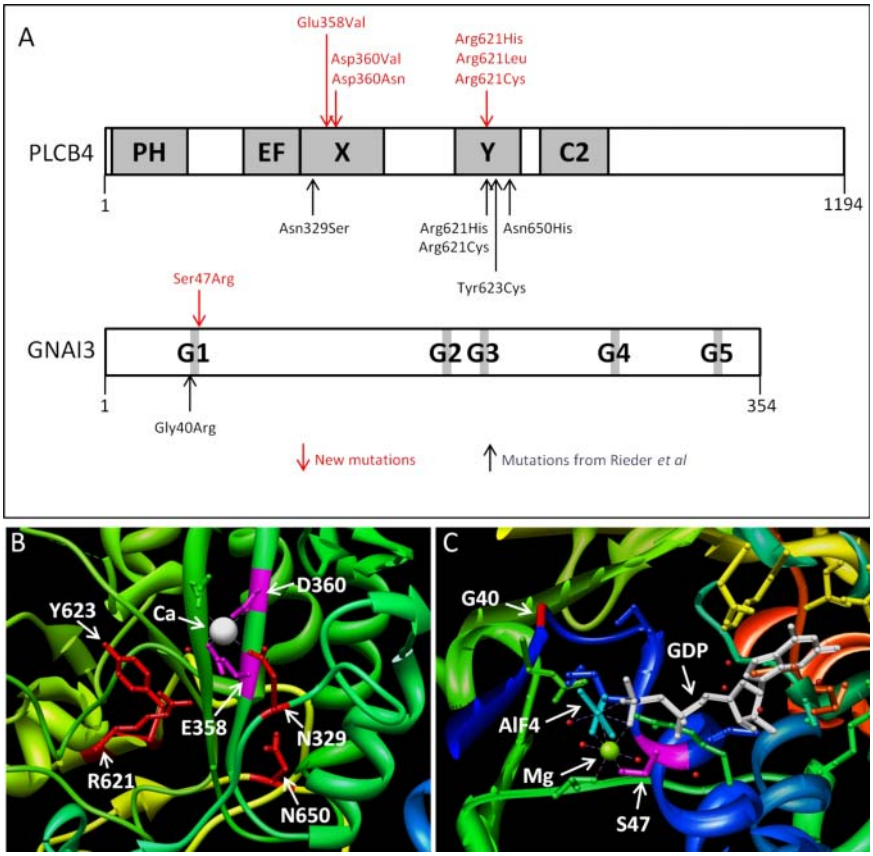

Figure 5 (A) distribution of mutations in PLCB4 and GNAI3 relative to domain structure. PLCB4 domains in grey: PH (pleckstrin homology), EF (EF hand-like), X and Y (catalytic), C2. GNAI3 domains in grey: boxes G1–G5. Mutations reported here are in red above each protein, and those reported in Rieder *et al*[24] are in black below. (B) mapping of mutated PLCB4 amino acids to the PLCB3 crystal structure. Residues previously reported as mutated[24] (Asn329, Arg621, Tyr623, Asn650) are in red, and those reported here (Glu358 and Asp360) are in magenta. Note that the numbering of these six residues refers to their position in the PLCB4 sequence, not PLCB3, but each of the six amino acids is identical at the homologous position in PLCB3. Calcium (Ca) is in white. (C) mapping of mutated amino acids to the GNAI3 crystal structure. The residue previously reported as mutated[24] (Gly40) is in red, the residue mutated in case 7 of this report (Ser47) is in magenta, GDP is in white, aluminium tetrafluoride (AlF4) is in cyan and magnesium (Mg) is in green. This figure is only reproduced in colour in the online version.

mutant function as dominant negatives,[29] and from a report of a *PLCD4* splice variant that produces an isoform capable of dominantly interfering with other PLC family members.[42] The phenotype, or lack thereof, of individuals with heterozygous *PLCB4* deletions or frameshift or stop mutations was not described by Rieder *et al*.[24] Individuals reported here, with heterozygous deletions of all or part of *PLCB4*, but without obvious features of ACS, provide strong evidence that the ACS-associated point mutations act as dominant negative rather than haploinsufficient alleles. In addition to the parents of case 8, we report two patients via DECIPHER, with deletions (likely heterozygous) that remove wholly or partly *PLCB4*, without leading to ACS. A series of five patients with overlapping microdeletions on chr20p12.3 associated with variably penetrant Wolff–Parkinson–White syndrome, dysmorphic features and neurocognitive delay has recently been reported, and although *PLCB4* is contained within the two largest deletions (both apparently heterozygous), ears typical of ACS were not reported.[43–45] *JAG1*, haploinsufficiency of which causes Alagille syndrome is 1.16 Mb centromeric to *PLCB4*. A number of deletions (likely heterozygous) in Alagille syndrome patients remove both *JAG1* and *PLCB4*, but typical ACS phenotypes were not reported in these cases.[46–48]

A range of mostly neurological phenotypes have been described in *Plcb4* knockout mice, including absence seizures, locomotor ataxia, defects in visual responses and processing, disruption of sleep sequence, increased anxiety and impaired fear extinction.[49–56] However, craniofacial defects have not been reported in *Plcb4* homozygous null mice. One hypothesis to explain the difference in phenotype between the missense mutations in humans and complete loss of function in mice would be that the mutant human PLCB4 protein dominantly interferes with multiple PLCB family members, and as noted above, this is supported by the evidence from the *plcb3* mutations in zebrafish and from studies of a *PLCD4* splice variant.[29 42] However, the finding of classical ACS craniofacial features in a patient with homozygous loss of *PLCB4* indicates that dominant interference with other PLCB family members is not necessary to produce the phenotype in humans. Indeed, the homozygous deletion case suggests that in the point mutation cases, dominant negative mutant PLCB4 only interferes with its wild-type PLCB4 counterpart in humans. Other possible reasons for the apparent discrepancy between human and mouse phenotypes could be that mice are better able to genetically compensate for the loss of *Plcb4*, or that subtle craniofacial defects do exist in the *Plcb4* null mice, but are yet to be appreciated.

The only mutation previously reported in GNAI3 in ACS patients was Gly40Arg, occurring in two unrelated cases, with the mutation inherited from an affected parent in one case and from an unaffected parent in the other.[24] Here we have identified a second GNAI3 mutation, Ser47Arg. Gly40 and Ser47 of GNAI3 corresponding to the first and last amino acids of the G1 box, one of five highly conserved motifs (G1–G5; figure 5A) involved in guanosine diphosphate (GDP)/guanosine triphosphate (GTP) binding by rat sarcoma (RAS) superfamily and G α proteins.[57] All 16 human G α proteins conform to the G1 box consensus of GXXXSGKS. The hydroxyl of the final serine of the G1 box is involved in the coordination of magnesium during GTP binding by G α proteins.[39] A mutation of the equivalent G1 box serine in HRAS (Ser17Asn) was shown to function as a dominant negative with growth-inhibitory properties,[58 59] and subsequently a mutation at this position has been engineered in many RAS superfamily members and G α proteins, with consequent dominant negative effects (reviewed in Barren and Artemyev[60]). It was suggested by Rieder *et* al,[24] that the

GNAI3 Gly40Arg mutation in two ACS patients represents a gain-of-function mutation, however, we suggest that Ser47Arg is more likely a dominant negative, based on the in vitro data for other GTP-binding proteins mutated at this position. The *GNAI3* mutation identified here was inherited from a father who was only mildly affected, consistent with the extreme phenotypic variability within families that occurs in other *GNAI3* or *PLCB4* mutation-positive cases. A similar phenomenon has been reported for other craniofacial disorders, for example, the non-penetrance for *POLR1D* mutations in some cases of Treacher Collins syndrome.[61]

Following exome sequencing of a series of ACS patients, Rieder *et al*[24] were unable to identify *PLCB4* or *GNAI3* mutations in only one case (A001). However, a private missense mutation was identified in each of *DOCK1* and *DOCK6* in this patient. Given that *DOCK* genes code for guanine nucleotide exchange factors,[62] and are therefore potential regulators of the G-protein-dependent pathway disrupted in ACS, it was proposed that these mutations may be responsible for ACS in patient A001, despite the absence of parental data. However, several arguments can be made against the putative involvement of *DOCK1* and *DOCK6* in ACS. Neither the DOCK1 nor DOCK6 mutation in patient A001 falls within the known domains of each protein ((http://www.uniprot.org/uniprot/Q14185) and (http://www.uniprot.org/uniprot/Q96HP0)). Recessive truncating mutations have been identified in *DOCK6* as a cause of Adams–Oliver syndrome—the major features of this syndrome are digit truncations and scalp hypoplasia, but no craniofacial or ear phenotypes were reported in *DOCK6*-mutant patients, and no phenotypes were reported for their heterozygous parents.[63] Murine *Dock6* does not appear to be strongly expressed in the proximal mandible or external ear at several stages of embryonic development, as judged by the whole-mount in situ hybridisation images in Shaheen *et al*.[63] *DOCK1* falls within the smallest region of overlap of several 10q deletions, and although craniofacial dysmorphism is a component of the associated 10q deletion syndrome,[64] to our knowledge, auricular defects of the ACS type have not been reported. For these reasons we did not sequence *DOCK1* and *DOCK6* in the *PLCB4*/*GNAI3* mutation-negative patients reported here.

Whether IQME is genetically distinct from ACS, or whether it represents variable expression of the same disorder remains unknown. Indeed, we identified a *PLCB4* mutation in a case previously reported as having IQME,[18] however, in our opinion, the lower jaw is mildly dysplastic in two members of that family. Conversely, we sequenced *PLCB4* and *GNAI3* in two familial cases of IQME, without overt signs of mandibular hypoplasia, and we did not identify any mutations.

Within the ACS literature, postauricular tags have been reported in a small number of cases.[2 3 9 33] We have shown here that the presence of a postauricular tag is a very strong indication of a *PLCB4* mutation. All cases in this report with a postauricular tag have either a mutation at Arg621 or a homozygous deletion within *PLCB4*. Note that the position of the postauricular tag in the *PLCB4* mutation-positive cases presented here is highly stereotypic, falling just above the lobe-helix junction. Although preauricular tags have been reported as a feature of several syndromes (perhaps most frequently in OAVS/GS), we are unaware of syndromes other than ACS with recurrence of postauricular tags. Although it has been claimed in the ACS literature that preauricular tags can occur as part of the phenotype, the evidence for this appears limited: preauricular tags were stated for individual IV-6 in Storm *et al*,[3] but from the image in that article, we suggest that the preauricular tag may be a dysplastic tragus or antitragus; and for individual IV-3 in Masotti *et al*,[2] although a classic postauricular tag is evident, the nature of the preauricular tag(s) is less clear. Along with the ear dysmorphology itself (see below), a post- versus a preauricular tag may be a useful feature in differentiating between ACS and other branchial arch anomalies.

It has been suggested that the auricular phenotype in ACS patients varies widely, and a recent report expanded the spectrum of ACS-associated anomalies to include ear phenotypes that might otherwise fall within OAVS/GS or other branchial arch syndromes.[30] For some mutation-positive individuals in the familial cases of the present report, an auricular phenotype was non-penetrant, but when present, the auricular dysplasia in almost all cases consisted of an abnormal junction between the lobe and helix, ranging from a small indentation to a deep cleft. One exception to this was the father of case 5, who presented an overfolded helix as the only auricular dysmorphology, and an overfolded helix has been reported in other ACS cases.[2 3] We sequenced all of *GNAI3* and the catalytic domain of *PLCB4* in five of the cases reported in McGowan *et al*,[30] and in 10 patients with ear and craniofacial features consistent with OAVS/GS or with isolated pharyngeal arch anomalies, but no clearly pathogenic mutations were identified. None of the patients described in McGowan *et al*[30] display the indentation or cleft between the helix and lobe that is characteristic of *PLCB4*/*GNAI3* mutation-positive ACS cases. In some of the former cases, a cleft occurs between the tragus and antitragus. Based on the model whereby six auricular hillocks surrounding the first pharyngeal cleft give rise to specific portions of the external ear,[65] it can be speculated that the boundary between the helix and lobe arises from the fusion of the fifth and sixth hillocks, while the tragus-anti-tragus boundary would arise from fusion across the first pharyngeal cleft. Our genotyping analysis supports the idea that the auricular phenotype in the patients reported in McGowan *et al*[30] is caused by disruption of molecular and embryonic events distinct from those causing *PLCB4*/*GNAI3*-related ACS. We conclude that the auricular phenotype of *PLCB4*/*GNAI3* mutation-positive ACS is in fact highly specific (notwithstanding the existence of both mild and severe forms within families), and distinguishable from other human ear dysplasias.

Author affiliations
[1]INSERM U781, Hôpital Necker-Enfants Malades and Université Paris Descartes–Sorbonne Paris Cité, Institut Imagine, Paris, France
[2]Centre de référence des surdités génétiques, Service de génétique médicale, Hôpital d'Enfants Armand-Trousseau AP-HP, Paris, France
[3]Department of Genetics, University of Groningen, University Medical Center Groningen, Groningen, the Netherlands
[4]Northern Genetics Service, Newcastle upon Tyne Hospitals NHS Foundation Trust, Newcastle Upon Tyne, UK
[5]Department of Genetics, Sultan Qaboos University Hospital, Muscat, Oman
[6]Service de Génétique Clinique, Hôpital Jeanne de Flandre, CHRU Lille, France
[7]Center for Tissue and Cell Sciences, Seattle Children's Research Institute, Seattle, USA
[8]West Midlands Regional Genetics Service, Birmingham, UK
[9]North East Thames Regional Genetics Service, Great Ormond Street Hospital, London, UK
[10]North Scotland Regional Genetics Service, Ashgrove House, Aberdeen, UK
[11]Laboratoire de génétique chromosomique, Hôpital St Vincent de Paul, Lille, France
[12]Institute of Human Genetics, Medical University of Graz, Graz, Austria
[13]Respiratory Medicine, Great Ormond Street Hospital, London, UK
[14]Centre de Référence des Malformations Cranio-maxillo-faciales Rares, CHRU Lille, France
[15]AP-HP, Département de Génétique, Hôpital Necker-Enfants Malades, Paris, France
[16]School of Medicine, University of Glasgow, Yorkhill Hospital, Glasgow, UK
[17]Institute for Medical and Molecular Genetics, La Paz University Hospital, Madrid, Spain
[18]Clinical and Molecular Genetics, Institute of Child Health, UCL, London, UK
[19]Department of Plastic and Reconstructive Surgery, Copenhagen University Hospital, Rigshospitalet, Denmark

[20]Department of Oral and Maxillofacial Surgery, Kennemer Gasthuis, Haarlem, The Netherlands
[21]Service de Pédiatrie Générale, Université Paris Descartes, Hôpital Necker-Enfants Malades, Paris, France
[22]INSERM UMR-S587 and Pediatric Otolaryngology Department, Armand-Trousseau Children's Hospital, AP-HP, Paris 6 University, Paris, France
[23]Service de Chirurgie Maxillo-Faciale et Plastique, CRMR des Malformations de la Face et de la Cavité Buccale, Hôpital Necker-Enfants Malades, AP-HP, Paris, France
[24]Université Paris 5, UFR de Médecine Paris-Descartes, Paris, France
[25]Centre de Recherche des Cordeliers, UMR S 872, Paris, France
[26]Department of Pediatrics and Adolescence Medicine, Medical University of Graz, Graz, Austria
[27]Service d'ORL Pediatrique, Hôpital Necker-Enfants Malades, AP-HP, Université Paris 5, Paris, France
[28]AP-HP, Service d'Imagerie Pédiatrique, Hôpital Necker-Enfants Malades, Paris, France
[29]Laboratoire d'Anatomie, Université Paris-Descartes, Paris, France
[30]Department of Clinical Genetics, Free University Medical Center, Amsterdam, The Netherlands
[31]Genetics Unit, MassGeneral Hospital for Children, Boston, Massachusetts, USA
[32]Department of Oral and Maxillofacial Surgery, Massachusetts General Hospital, Boston, Massachusetts, USA
[33]Pediatric Genetics, Schneider Children's Medical Center of Israel and Raphael Recanati Genetics Institute, Rabin Medical Center, Beilinson Campus, Petah Tikva, Israel
[34]Sackler Faculty of Medicine, Tel Aviv University, Tel Aviv, Israel;
[35]Felsenstein Medical Research Center, Rabin Medical Center, Petah Tikva, Israel
[36]Department of Pediatrics, University of Washington and Seattle Children's Hospital Craniofacial Center, Seattle, Washington, USA

Acknowledgements This work was supported by funding from the Ecole de l'Inserm Liliane Bettencourt (AV), the Jean Renny Endowment for Craniofacial Research (MLC), E-Rare CRANIRARE (SL) and the Fondation pour la Recherche Médicale (JA).

Contributors CTG, AV, SSP, AO, MS-B, EBB, MO, RP, BD and MS performed genetic analysis. SM, EG, AH, AA, MH-E, BS-R, AS, RM, FP, MRS, PA, DK, PP, J-PB, EST, SG-M, MB-G, PL, BAM, VA, FD, M-PV, CR-F, VC, SP, YM, SB, YMCH, AM, LJ, PK, AL, LBK, LB-V, LW, MLC, SL and JA diagnosed or treated patients. CTG, AV and JA wrote the manuscript.

Competing interests None.

Ethics approval CPP Ile-de-France II.

Patient consent Obtained.

Provenance and peer review Not commissioned; externally peer reviewed.

REFERENCES

1 Kokitsu-Nakata NM, Zechi-Ceide RM, Vendramini-Pittoli S, Tavares VL Romanelli, Passos-Bueno MR, Guion-Almeida ML. Auriculo-condylar syndrome. Confronting a diagnostic challenge. *Am J Med Genet A* 2011;158A:59–65.
2 Masotti C, Oliveira KG, Poerner F, Splendore A, Souza J, Rda S Freitas, Zechi-Ceide R, Guion-Almeida ML, Passos-Bueno MR. Auriculo-condylar syndrome: mapping of a first locus and evidence for genetic heterogeneity. *Eur J Hum Genet* 2008;16:145–52.
3 Storm AL, Johnson JM, Lammer E, Green GE, Cunniff C. Auriculo-condylar syndrome is associated with highly variable ear and mandibular defects in multiple kindreds. *Am J Med Genet A* 2005;138A:141–5.
4 Ozturk S, Sengezer M, Isik S, Gul D, Zor F. The correction of auricular and mandibular deformities in auriculo-condylar syndrome. *J Craniofac Surg* 2005;16:489–92.
5 Guion-Almeida ML, Zechi-Ceide RM, Vendramini S, Kokitsu-Nakata NM. Auriculo-condylar syndrome: additional patients. *Am J Med Genet* 2002;112:209–14.
6 Divizia MT, Cordone A, Bado M, Rosaia L, Silengo M Cirillo, Ravazzolo R, Lerone M. Auriculo-condylar syndrome or new syndrome? *Clin Dysmorphol* 2002;11:143–4.
7 Priolo M, Lerone M, Rosaia L, Calcagno EP, Sadeghi AK, Ghezzi F, Ravazzolo R, Silengo M. Question mark ears, temporo-mandibular joint malformation and hypotonia: auriculo-condylar syndrome or a distinct entity? *Clin Dysmorphol* 2000;9:277–80.
8 Guion-Almeida ML, Kokitsu-Nakata NM, Zechi-Ceide RM, Vendramini S. Auriculo-condylar syndrome: further evidence for a new disorder. *Am J Med Genet* 1999;86:130–3.
9 Gerkes EH, van Ravenswaaij CM, van Essen AJ. Question mark ears and post-auricular tags. *Eur J Med Genet* 2008;51:264–7.
10 Al-Qattan MM. Cosman (question mark) ear: congenital auricular cleft between the fifth and sixth hillocks. *Plast Reconstr Surg* 1998;102:439–41.
11 Takato T, Takeda H, Kamei M, Uchiyama K. The question mark ear (congenital auricular cleft): a familial case. *Ann Plast Surg* 1989;22:69–73.
12 Fumiiri M, Hyakusoku H. Congenital auricular cleft. *Plast Reconstr Surg* 1983;71:249–50.
13 Uuspaa V. Combined bilateral external ear deformity and hypoplastic mandible. Case report. *Scand J Plast Reconstr Surg* 1978;12:165–7.
14 Jampol M, Repetto G, Keith DA, Curtin H, Remensynder J, Holmes LB. New syndrome? Prominent, constricted ears with malformed condyle of the mandible. *Am J Med Genet* 1998;75:449–52.
15 Erlich MS, Cunningham ML, Hudgins L. Transmission of the dysgnathia complex from mother to daughter. *Am J Med Genet* 2000;95:269–74.
16 Posso CM, Wolff GA, Suarez LD. Question mark ear deformity: a combined method for correction. *Aesthetic Plast Surg* 2011;35:646–9.
17 Pan B, Jiang H, Zhao Y, Lin L, Guo D, Zhuang H. Clinical analysis, repair and aetiology of question mark ear. *J Plast Reconstr Aesthet Surg* 2010;63:28–35.
18 Shkalim V, Eliaz N, Linder N, Merlob P, Basel-Vanagaite L. Autosomal dominant isolated question mark ear. *Am J Med Genet A* 2008;146A:2280–3.
19 Vayvada H, Karaca C, Menderes A, Yilmaz M. Question mark ear deformity and a modified surgical correction method: a case report. *Aesthetic Plast Surg* 2005;29:251–4; discussion 5.
20 Brodovsky S, Westreich M. Question mark ear: a method for repair. *Plast Reconstr Surg* 1997;100:1254–7.
21 Cosman B, Bellin H, Crikelair GF. The Question Mark ear. *Plast Reconstr Surg* 1970;46:454–7.
22 Baker PA, Aftimos S, Anderson BJ. Airway management during an EXIT procedure for a fetus with dysgnathia complex. *Paediatr Anaesth* 2004;14:781–6.
23 Greig AV, Podda S, Thorne CH, McCarthy JG. The question mark ear in patients with mandibular hypoplasia. *Plast Reconstr Surg* 2012;129:368e–9e.
24 Rieder MJ, Green GE, Park SS, Stamper BD, Gordon CT, Johnson JM, Cunniff CM, Smith JD, Emery SB, Lyonnet S, Amiel J, Holder M, Heggie AA, Bamshad MJ, Nickerson DA, Cox TC, Hing AV, Horst JA, Cunningham ML. A human homeotic transformation resulting from mutations in PLCB4 and GNAI3 causes auriculocondylar syndrome. *Am J Hum Genet* 2012;90:907–14.
25 Stuffken MJ, Tuinzing DB. Dysgnathia complex, a rare deviation. *Ned Tijdschr Tandheelkd* 2008;115:394–6.
26 Vincent RW, Ryan RF, Longenecker CG. Malformation of ear associated with urogenital anomalies. *Plast Reconstr Surg Transplant Bull* 1961;28:214–20.
27 Park C. Correction of the unilateral question mark ear. *Plast Reconstr Surg* 1998;101:1620–3.
28 Clouthier DE, Garcia E, Schilling TF. Regulation of facial morphogenesis by endothelin signaling: insights from mice and fish. *Am J Med Genet A* 2010;152A:2962–73.
29 Walker MB, Miller CT, Swartz ME, Eberhart JK, Kimmel CB. Phospholipase C, beta 3 is required for Endothelin1 regulation of pharyngeal arch patterning in zebrafish. *Dev Biol* 2007;304:194–207.
30 McGowan R, Murday V, Kinning E, Garcia S, Koppel D, Whiteford M. Novel features in auriculo-condylar syndrome. *Clin Dysmorphol* 2011;20:1–10.
31 Soundararajan M, Willard FS, Kimple AJ, Turnbull AP, Ball LJ, Schoch GA, Gileadi C, Fedorov OY, Dowler EF, Higman VA, Hutsell SQ, Sundstrom M, Doyle DA, Siderovski DP. Structural diversity in the RGS domain and its interaction with heterotrimeric G protein alpha-subunits. *Proc Natl Acad Sci USA* 2008;105:6457–62.
32 Waldo GL, Ricks TK, Hicks SN, Cheever ML, Kawano T, Tsuboi K, Wang X, Montell C, Kozasa T, Sondek J, Harden TK. Kinetic scaffolding mediated by a phospholipase C-beta and Gq signaling complex. *Science* 2010;330:974–80.
33 Hunter A, Frias JL, Gillessen-Kaesbach G, Hughes H, Jones KL, Wilson L. Elements of morphology: standard terminology for the ear. *Am J Med Genet A* 2009;149A:40–60.
34 Conrad DF, Bird C, Blackburne B, Lindsay S, Mamanova L, Lee C, Turner DJ, Hurles ME. Mutation spectrum revealed by breakpoint sequencing of human germline CNVs. *Nat Genet* 2010;42:385–91.
35 Dettlaff-Swiercz DA, Wettschureck N, Moers A, Huber K, Offermanns S. Characteristic defects in neural crest cell-specific Galphaq/Galpha11- and Galpha12/Galpha13-deficient mice. *Dev Biol* 2005;282:174–82.
36 Ivey K, Tyson B, Ukidwe P, McFadden DG, Levi G, Olson EN, Srivastava D, Wilkie TM. Galphaq and Galpha11 proteins mediate endothelin-1 signaling in neural crest-derived pharyngeal arch mesenchyme. *Dev Biol* 2003;255:230–7.
37 Offermanns S, Zhao LP, Gohla A, Sarosi I, Simon MI, Wilkie TM. Embryonic cardiomyocyte hypoplasia and craniofacial defects in G alpha q/G alpha 11-mutant mice. *EMBO J* 1998;17:4304–12.
38 Sato T, Kawamura Y, Asai R, Amano T, Uchijima Y, Dettlaff-Swiercz DA, Offermanns S, Kurihara Y, Kurihara H. Recombinase-mediated cassette exchange reveals the selective use of Gq/G11-dependent and -independent endothelin 1/endothelin type A receptor signaling in pharyngeal arch development. *Development* 2008;135:755–65.
39 Birnbaumer L, Zurita AR. On the roles of Mg in the activation of G proteins. *J Recept Signal Transduct Res* 2010;30:372–5.
40 Nezarati MM, Aftimos S. Microtia, severe micrognathia and absent ossicles: auriculo-condylar syndrome or new entity? *Clin Dysmorphol* 2007;16:9–13.

41 Gaultier C, Amiel J, Dauger S, Trang H, Lyonnet S, Gallego J, Simonneau M. Genetics and early disturbances of breathing control. *Pediatr Res* 2004;55:729–33.
42 Nagano K, Fukami K, Minagawa T, Watanabe Y, Ozaki C, Takenawa T. A novel phospholipase C delta4 (PLCdelta4) splice variant as a negative regulator of PLC. *J Biol Chem* 1999;274:2872–9.
43 Lalani SR, Thakuria JV, Cox GF, Wang X, Bi W, Bray MS, Shaw C, Cheung SW, Chinault AC, Boggs BA, Ou Z, Brundage EK, Lupski JR, Gentile J, Waisbren S, Pursley A, Ma L, Khajavi M, Zapata G, Friedman R, Kim JJ, Towbin JA, Stankiewicz P, Schnittger S, Hansmann I, Ai T, Sood S, Wehrens XH, Martin JF, Belmont JW, Potocki L. 20p12.3 microdeletion predisposes to Wolff-Parkinson-White syndrome with variable neurocognitive deficits. *J Med Genet* 2009;46:168–75.
44 Anad F, Burn J, Matthews D, Cross I, Davison BC, Mueller R, Sands M, Lillington DM, Eastham E. Alagille syndrome and deletion of 20p. *J Med Genet* 1990;27:729–37.
45 Shohat M, Herman V, Melmed S, Neufeld N, Schreck R, Pulst S, Graham JM Jr, Rimoin DL, Korenberg JR. Deletion of 20p 11.23—pter with normal growth hormone-releasing hormone genes. *Am J Med Genet* 1991;39:56–63.
46 Robert ML, Lopez T, Crolla J, Huang S, Owen C, Burvill-Holmes L, Stumper O, Turnpenny PD. Alagille syndrome with deletion 20p12.2-p12.3 and hypoplastic left heart. *Clin Dysmorphol* 2007;16:241–6.
47 Kamath BM, Thiel BD, Gai X, Conlin LK, Munoz PS, Glessner J, Clark D, Warthen DM, Shaikh TH, Mihci E, Piccoli DA, Grant SF, Hakonarson H, Krantz ID, Spinner NB. SNP array mapping of chromosome 20p deletions: genotypes, phenotypes, and copy number variation. *Hum Mutat* 2009;30:371–8.
48 Le Gloan L, Pichon O, Isidor B, Boceno M, Rival JM, David A, Le Caignec C. A 8.26Mb deletion in 6q16 and a 4.95Mb deletion in 20p12 including JAG1 and BMP2 in a patient with Alagille syndrome and Wolff-Parkinson-White syndrome. *Eur J Med Genet* 2008;51:651–7.
49 Cheong E, Zheng Y, Lee K, Lee J, Kim S, Sanati M, Lee S, Kim YS, Shin HS. Deletion of phospholipase C beta4 in thalamocortical relay nucleus leads to absence seizures. *Proc Natl Acad Sci USA* 2009;106:21912–17.
50 Jiang H, Lyubarsky A, Dodd R, Vardi N, Pugh E, Baylor D, Simon MI, Wu D. Phospholipase C beta 4 is involved in modulating the visual response in mice. *Proc Natl Acad Sci USA* 1996;93:14598–601.
51 Kano M, Hashimoto K, Watanabe M, Kurihara H, Offermanns S, Jiang H, Wu Y, Jun K, Shin HS, Inoue Y, Simon MI, Wu D. Phospholipase cbeta4 is specifically involved in climbing fiber synapse elimination in the developing cerebellum. *Proc Natl Acad Sci USA* 1998;95:15724–9.
52 Kim D, Jun KS, Lee SB, Kang NG, Min DS, Kim YH, Ryu SH, Suh PG, Shin HS. Phospholipase C isozymes selectively couple to specific neurotransmitter receptors. *Nature* 1997;389:290–3.
53 Xue T, Do MT, Riccio A, Jiang Z, Hsieh J, Wang HC, Merbs SL, Welsbie DS, Yoshioka T, Weissgerber P, Stolz S, Flockerzi V, Freichel M, Simon MI, Clapham DE, Yau KW. Melanopsin signalling in mammalian iris and retina. *Nature* 2011;479:67–73.
54 Ikeda M, Hirono M, Sugiyama T, Moriya T, Ikeda-Sagara M, Eguchi N, Urade Y, Yoshioka T. Phospholipase C-beta4 is essential for the progression of the normal sleep sequence and ultradian body temperature rhythms in mice. *PLoS One* 2009;4:e7737.
55 Shin J, Gireesh G, Kim SW, Kim DS, Lee S, Kim YS, Watanabe M, Shin HS. Phospholipase C beta 4 in the medial septum controls cholinergic theta oscillations and anxiety behaviors. *J Neurosci* 2009;29:15375–85.
56 Lee S, Ahmed T, Kim H, Choi S, Kim DS, Kim SJ, Cho J, Shin HS. Bidirectional modulation of fear extinction by mediodorsal thalamic firing in mice. *Nat Neurosci* 2012;15:308–14.
57 Wennerberg K, Rossman KL, Der CJ. The Ras superfamily at a glance. *J Cell Sci* 2005;118:843–6.
58 Feig LA, Cooper GM. Inhibition of NIH 3T3 cell proliferation by a mutant ras protein with preferential affinity for GDP. *Mol Cell Biol* 1988;8:3235–43.
59 Feig LA. Tools of the trade: use of dominant-inhibitory mutants of Ras-family GTPases. *Nat Cell Biol* 1999;1:E25–7.
60 Barren B, Artemyev NO. Mechanisms of dominant negative G-protein alpha subunits. *J Neurosci Res* 2007;85:3505–14.
61 Dauwerse JG, Dixon J, Seland S, Ruivenkamp CA, van Haeringen A, Hoefsloot LH, Peters DJ, Boers AC, Daumer-Haas C, Maiwald R, Zweier C, Kerr B, Cobo AM, Toral JF, Hoogeboom AJ, Lohmann DR, Hehr U, Dixon MJ, Breuning MH, Wieczorek D. Mutations in genes encoding subunits of RNA polymerases I and III cause Treacher Collins syndrome. *Nat Genet* 2011;43:20–2.
62 Cote JF, Vuori K. GEF what? Dock180 and related proteins help Rac to polarize cells in new ways. *Trends Cell Biol* 2007;17:383–93.
63 Shaheen R, Faqeih E, Sunker A, Morsy H, Al-Sheddi T, Shamseldin HE, Adly N, Hashem M, Alkuraya FS. Recessive mutations in DOCK6, encoding the guanidine nucleotide exchange factor DOCK6, lead to abnormal actin cytoskeleton organization and Adams-Oliver syndrome. *Am J Hum Genet* 2011;89:328–33.
64 Yatsenko SA, Kruer MC, Bader PI, Corzo D, Schuette J, Keegan CE, Nowakowska B, Peacock S, Cai WW, Peiffer DA, Gunderson KL, Ou Z, Chinault AC, Cheung SW. Identification of critical regions for clinical features of distal 10q deletion syndrome. *Clin Genet* 2009;76:54–62.
65 Passos-Bueno MR, Ornelas CC, Fanganiello RD. Syndromes of the first and second pharyngeal arches: A review. *Am J Med Genet A* 2009;149A:1853–9.

Supplementary Table 1. Sequencing primers. *PLCB4* primer pairs a, b, c and d were used for amplification of intronic products during the deletion breakpoint mapping for case 8.

Exon	Forward primer	Reverse primer
PLCB4		
EX 3	TCTGCAAACACAGAAATGCGAAG	AAAGATGTTCTTACTTATGTCAAAG
EX 4	TTTCTAATTTGTTTAGAAGCTCAGC	GGGTAGGGTTCATCAACAGCAC
EX 5	GAAATTTTTGCCAAGCAGTTTGCC	GTAGCCTGGATACAAAGAGTGAG
EX 6	CAGGTTTTAGAATAATGCTAGGTG	GATTTTCTACAGAAACATGTCAGC
EX 7	GCTGTGTGACAGGAAAGGGAC	CAACTCCAAGGTCAGGAGCATG
EX 8	AAGTTCTTAACAGAATTGAAGCTG	GCATTTAACACACAAATACTTGTG
EX 9	GAGGTAATTTTATTCTCCTCTTCC	ATCTAGCTCATTACATATGAGAAG
EX 10	GTCTTCACTGTGCTTCATGACC	CCAACATACTCTATTAAAATAGGAC
EX 11	GAATTATCATCAACAAATGTCAAC	AGCAAAGCGAATAAGGGCATATG
EX 12	GTAATTATAAACATGACAGTCTAG	ATGGCTCAGGGAGTTGCAAAGC
EX 13	CTCTTATAATTTAAGCTGCCTCAG	CTGATTACTATTTCCTGTTTTTCAG
EX 14	TTTTCTGTTCTGGAAGAAAACAAC	ATGCTTGAGAAAATGAATCATTTG
EX 15	GGAATTGACTTTCTGAAAGACTC	GTACTTCACAAAACAAACTATTCAG
EX 16	AAGTGAGAATCTTTAATTGCCTAG	GAAGATCTTTAGCATTAGTCCTC
EX 17	GTGTTGGGTTGCATCACTCCCAG	GTACCTGTAACATCACCCCTAC
EX 18	CTCCTCAGTGTCGATCTCAAGG	CAGCCTGGTTTTCTTATTTAAAAAG
EX 19	TAGCATCCTTTTTCTCTAAAAGTGC	GCAATTTAGAAGGGGAATTATAGG
EX 20	CATCAGTAATGTCCCACCTTAGC	CAGTGAAGAAAATGCCTTACTGC
a	CATGGATTACATCATCCAACTAAG	CACTCTAGAATGTAAGCAACATAC
EX 21	TTGAGGAAGAAAAAGCCTTTACC	AATAAGGTGAGGTGGAACAGCC
EX 22	TGACATGATAATGTAGCATTAGC	ACCACCAGAATGAGATATTAGCC
EX 23	GTCATTGTTGGCCTAGACCTTTG	CAATAACACATTGCTTTGCCATATG
EX 24	CTGTGGGCCTAGGAGCAATCTG	CCTCAAACCCAGCTTAAATTCTG
b	GCACATTTCTGTGCAAAAGTGAG	GCATGTTAGACAGCTGATGGC
c	GAGGACTGCATTTCTTAAAGAGG	CCTCTGAATCATAAAATGTCATAC
d	CCCTTTTGGGTTGTATTTTAACAG	CCTCACTACACAATGTCTGCC
EX 25	GCTCCTGTGTTACAGATGGAG	GGAATCTTAAGTCAAAGTTGTG
EX 26	GAAATTCCTGCTCCCACCCAAAAG	AGAAGATGTTGTCGGTTGAATAAG
EX 27	CATCAGGGAACATTTAAGAACAGC	GCAGCATTAGCAGGAATAGACAG
EX 28	GTGTGTCTTATGTCCTAGGAAAAG	CTATTGTTGAATTGATGAGCTCAG
EX 29	GTCTAGGAAGAGTATGGTAGAAG	TGTAAAAGGTTCTTTCCCACAAAG
EX 30/31	CATATGTAAAGCTGCTTCAAAGTC	GAGTTATTACTGTTAAGTGGTCTG
EX 32	CCTTGACTTTCTAAATGAAGACTC	ATCAAGTCAACACTAAGTTCTTCC
EX 33	AGCCATGACATCTCATATTTGATG	CTAGACCAGCTCTGGGCTACTG
EX 34	ACCAATTAAGTTGGTGGGAGGAAC	CATGTTGTACGTCAAATTGATTTCAC
EX 35	GCCACCCACCTCTAGAACTTTC	CCACAAGTGTTTTGCTGTCTCAG
EX 36/37	CAGAGAATTTGATGGAATATAGCTC	CCATGGCATGTGTATCCCAAAG
EX 38	TTTGCTTTTCTGTATATGGTTTTGC	CCTTCAGATATTAGTTATGACCAG
EX 39	GTGGTGACAGGATCATATTTATGG	TAAGGCATCACAAAGGAGAGTTG

Exon	Forward primer	Reverse primer
GNAI3		
EX 1	GGCGCTAAGGGAGCTGACGGAG	GATCCCTTTAGGGTCCTTTCCG
EX 2/3	GGTTTTCATCAATCTAGAGTTATC	TCTTGTTGCTTAAATTCATTTCCC
EX 4	GAAAAGGTCTCTGTAACAACACC	TCCTATAAACGTCTAAGAGTGTC
EX 5	GCCACTTAATAACTAGTAACAGG	AACCAAGGAATACTGCCCAGAG
EX 6	GTTGTCTTGTACTTTTAGCCAGG	GGTTGAATGAGGAAATGGATGC
EX 7	GCCATTTAGTGCTGCAAAACTTG	AAAAGGCAGTTTTATGAATGCCACC
EX 8	GTTCCCTCTCCATAAGTAAATGG	CAACACTCCACACTGTAGTAACTAG
PLCB3		
EX 9/10	CAGGGCAAGGGCTTGGCGACGG	CCCCAGGAGGAGTGGGGCTGT
EX 11	CAGCATGTCCTGGTTCCAGGTGG	CTGAGCAGTCCAACAGCACTG
EX 12/13	CGGCCACTGACATGTCCCGTAG	TGGGCTGGGGGTCTGGGATGAAG
EX 15/16	AGTGTGTATATAGTGCTGGGAAG	ACTGCCTGGATCTGCCCAAGCC
EX 17	GTCACAGGAGCACCTGGCTGAG	GACAGGGTCAGAGGTCCATTCAG
EX 18/19	GATGATCTCCCATTCCCCACATG	CCACCTGAGAGTCGGGGCGGTC
GNAQ		
EX 1	GAAGGCAGCTGCCCCGCAGGGC	AGGGCGGGAGGGTGTGTGTGCG
EX 2	CAAGAGGCTACTCGTGTTGTCAC	GTTAAATCCAAGGCATGGTATTTG
EX 3	AGTTCAATATCTATATTCCCTAAC	TATATGAAGGAAGGTGTTACCTG
EX 4	TTTCCTCCCTCAGGGATATGTC	TCTTCTTTACTTCTCTGTTAGGAC
EX 5	AAGAAGTAAGTTCACTCCATTCCC	GAGAATATTTTCCCTAAGTTTGTAAGTAG
EX 6	GCAAGGGCAGCAATGGTGCACTG	CGTATACAAAAGATGGGTTGGAC
EX 7	GCAAATTGTTTTCCACAGAAATAC	CAATGACACAGTATTTATTGAACC
GNA11		
EX 1	CGAGGCGGCTCCGGCCAGGGCC	GGCCCGACCCGGACAGGCAGGGC
EX 2	CAGCACGGCAGGGTCTGGGTAAG	TGGCAGCGCGGCCACCATGCTC
EX 3	GGCCAGCCGAGGCCTGGAAGAG	GGAGGCCTTCCCGAAGGGTCCC
EX 4	TGGGTGCTGTGTCCCTGTCCTG	CCCAAAGCACTGGGTGCGCAGG
EX 5/6	GGCTTGGGTGGGAGCCGTCCTG	GCCCCTCTCCCATATCAGCCC
EX 7	CTCATCCCCTGGGAGTGACAAAG	GGCCCGGACTCGGCAGCGCCAC

Supplementary Table 2. Primers used for microsatellite analysis during paternity testing and testing for homozygosity at the *PLCB4* locus.

Microsatellite	Forward primer	Reverse primer
Paternity testing		
D20S194	CCAGGATTCTTTCAGGCT	GCCAGAGTCCAACGCT
D11S4175	GGTGCAGGACTGCCTGT	CTGCCCAGCCAAACAT
D1S2696	AAAAATGAGTCCAGTAGAAGCCT	AGCCAGATTTACATCCCAG
D9S286	TGGAGTGCGCTCATAC	CCACCACCTACATGGC
D16S3024	ACATGCTGTGCCACCT	AGCTGCCAGTATATGGAGGA
D12S1597	AGACTGCCTGAGCCTGG	ACCTGATTTTAGTTGAATGCCC
D6S1572	CCTGAAATCATCCTGCAA	TTCTCTACAGTGACCAGCC
D8S1836	CCTTCATATCCTCCATACCC	GCTGACTCCGTCCTGTGT
D21S1903	GCTTGCTGAACTCACCTG	GCCTCCCAAAGTGCTC
D14S1023	TGCATTTCCCGTAGACATT	GACTCTTGTAGTTCTTTGAAGCC
D19S412	TGAGCGACAGAATGAGACT	ACATCTTACTGAATGCTTGC
D4S3038	GAAGACCAGCATTCGG	GGTTTAATACACAGTAATTGTTCA
PLCB4 homozygosity		
D20S851	ACTTCAAGTTATGTGTGGCACAA	GCCCAGACTCTGACACCTTT
D20S917	GATTTTGGTCTACGGTTTCCTTATT	ATCATTTGGGAAGTTTCCATT
BBS6	CTGTTTGGGAAGTTCTAGGAA	GCAAGAGATTAATGAACAGAAGAGGG